Mapping geological features in HRAM data using 2D steerable filters and its comparison to 2D wavelet transform

Hassan H. Hassan and John W. Peirce, GEDCO*

Summary

High **R**esolution **A**ero**M**agnetic (HRAM) maps display geological features of various shapes, orientations and magnitudes. Several techniques exist to enhance and map these geological features from HRAM data. These techniques include the FFT, wavelet transform, curvelet and ridgelet. Although these techniques provide powerful tools for extracting either linear, curvilinear or circular features from HRAM data, they fail to extract all these features in one run. For example, using wavelet analysis the horizontal, the vertical and the diagonal information in the data can be extracted from three different images. We believe that linear, curvilinear and circular features are important to map because they reflect certain geological structures such as fractures, faults, folds, impact structures and kimberlite pipes that might have significant impact on geophysical data interpretation. For this reason, we tested a new type of image enhancement technique based on steerable filters to map linear, curvilinear and circular features from HRAM data and compared the results to the results of wavelet transform. We tested the method on HRAM data from the Northeastern British Columbia (NEBC). The preliminary results of the test are very encouraging. We were able to detect curvilinear and circular features that did not appear on the results of the wavelet transform images.

Introduction

The HRAM data tested in this work was acquired over part of NEBC (Fig. 1). The survey was flown in 1996 by Sander Geophysics with a flight line spacing of 800 m oriented EW and a tie line spacing of 2400 m oriented NS. The survey was flown with a draped ground clearance of 120 m. GEDCO performed cultural editing on the survey data. Magnetic data profiles were examined and where magnetic anomalies correlated with known cultural artifacts the anomalies were carefully edited out of the profiles.

The test area is located at the border of the Foothills thrust belt with the Western Canada Sedimentary Basin (WCSB). The area intersects three main Precambrian litho-tectonic magnetic basement terranes (Fig. 2); Fort Simpson Magmatic Arc (1.84 – 1.88 Ga) at the center, Nahanni to the west, and Hottah (> 2.0 Ga) to the east.

The Precambrian basement terranes in the WCSB have been interpreted from the amplitude, texture and trends of the regional aeromagnetic data in conjunction with gravity data and isotopic age dating of Precambrian drill cores (Ross *et al*., 1994; Pilkington *et al*., 2000). The Fort Simpson Magmatic Arc Terrane has a distinctive NS trending magnetic high (Fig. 2) with ovoid internal structure. The Fort Simpson magnetic terrane is interpreted to represent a pre-collisional magmatic arc built upon the eastern margin of the Nahanni Terrane by a west-dipping subduction zone. At the completion of subduction between 1.84 Ga and 1.66 Ga, the Fort Simpson Arc collided with Hottah Terrane to the east, leading to the tectonic evolution of the Wopmay Orogen. The Fort Simpson Terrane is characterized by the presence of ferrimagnetic minerals, most likely magnetite, which has a sufficiently high susceptibility to produce of the high amplitude anomalies characteristic of this terrane. Such large magnetization is usually indicative of calc-alkaline igneous rocks associated with magmatic-arc environments. The Nahanni terrane which is associated with a magnetic low is interpreted as thinned Fort Simpson basement (Cook *et al*., 1999). According to Burwash (1957; 1989) the magnetic sources within the Nahanni Terrane are paramagnetic, i.e., comprise low-susceptibility silicate minerals, such as biotite, olivine, and amphiboles, which have low magnetic susceptibilities.

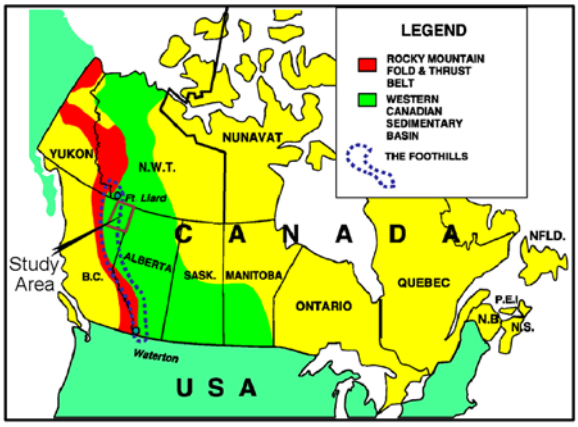

Figure 1. Index map showing the location of the study area.

The crystalline basement rocks of the WCSB have been extensively deformed over the last two billion years. Some of these deformations have affected the intra-sedimentary rocks and led to the formation of fractures, faults and folds

that often appear as linear and curvilinear features on the HRAM data. These lineaments play a major role in oil and gas exploration because they control structures in the intra-sedimentary section as well as in the crystalline basement rocks. For this reason, we consider mapping these features in HRAM data to be one of the most important stages in geological interpretation of an area.

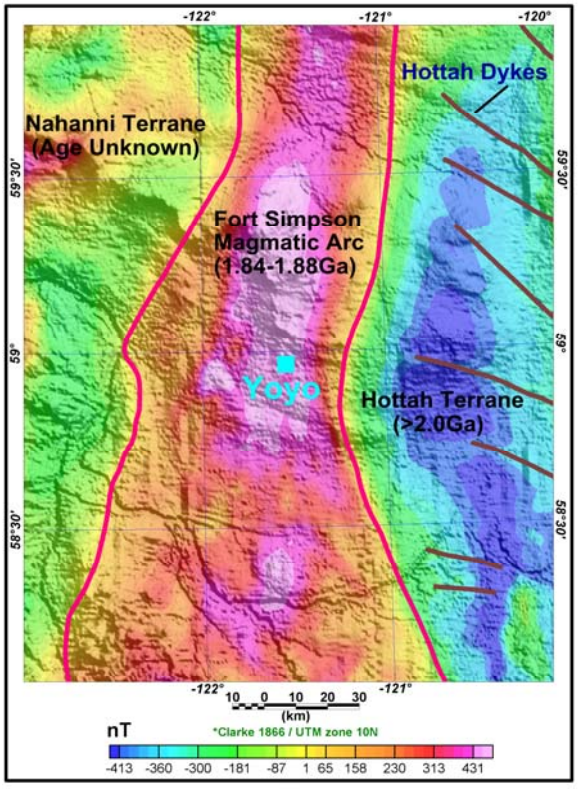

Figure 2. Reduced-to-pole total magnetic intensity grid of the test area draped on NE-shaded topography with the Precambrian magnetic terranes. The location of the largest gas field (Yoyo) discovered in 1962 is also plotted on this map.

Traditionally, features detection and mapping in HRAM data is carried out by visual inspection of a set of enhanced and filtered images of the total magnetic intensity. These filters (for example the horizontal gradient and the analytic signal) are carefully designed to image features that are associated with faults, fractures, and geological contacts. Going through this process thoroughly over a full range of wavelengths can be a very tedious operation. We have experimented in the past with alternative techniques such as wavelet analysis (Hassan, 2006). Wavelet analysis is good at mapping linear features but it is poor at mapping curvilinear and circular features. In this study we are testing steerable filters for the same purpose and compare it with the results of wavelet transform.

Methodology

Steerable filters were first introduced by Freeman and Adelson in 1991 and since then used widely by many researchers for edge detection, image enhancement and pattern recognition. In this work we adopt the technique described by Mathews and Unser (2004). The term 'steerable filter' is used to describe a class of filters in which a filter of arbitrary orientation is synthesized as a linear combination of a set of 'basis filters'. In addition to linear features, these basis filters are designed to detect curvilinear or circular features represented as edges or ridges in an image as illustrated in Figure 3.

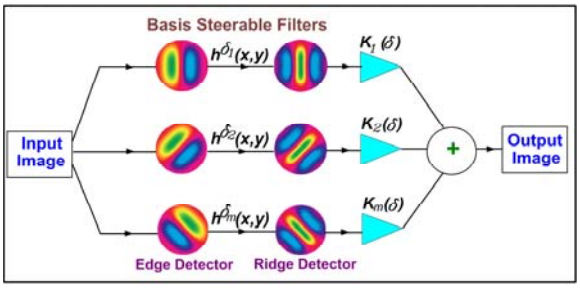

Figure 3. Principle of steerable filters (modified after Freeman and Adelson, 1991).

Freeman and Adelson (1991) proposed an efficient scheme for computing arbitrary rotations of 2-D steerable filters (Fig. 3). In this scheme an impulse function $h^{\theta a}(x,y)$ rotated by an arbitrary angle θa was formulated as a linear combination of basis functions $h^{\theta i}(x,y)$ as follows:

$$h^{\theta a}(x,y) = \sum_{i=1}^{m} K_i(\theta a) \cdot h^{\theta i}(x,y)$$

where $K_i(\theta a)$ are filter coefficients.

We tested the steerable filters, edge and ridge detectors, on the reduced-to-pole total magnetic intensity grid shown in Figure 4a.

In order to compare the results of the steerable filters with the results of wavelet transform we ran 2D discrete wavelet transform (DWT) on the reduced-to-pole total magnetic intensity grid (Fig. 4a). The 2D DWT (Daubechies, 1990; Chapin, 1997) decomposes an image into three components (horizontal, vertical and diagonal) using synthetic filter banks. In this work we used Haar wavelet with a base function of four.

Results

The results of steerable filters after skeletonization are shown in Figures 4b and 4c, respectively. Skeletonization is a process of converting the image into a binary form where we assign a value of one (black pixel) to the signal of interest (here the location of the lineaments) and a value of zero (white pixel) to the background based on a selected threshold value. The results in general of applying steerable filters are intriguing. Most of the features detected are continuous and highly coherent probably due to high signal/noise ratio.

The results of 2D wavelet analysis after skeletonization are shown in Figures 4d, 4e and 4f which reveal lineament information in four directions; E-W (Fig. 4d), N-S (Fig. 4e), NE-SW and NW-SE (Fig. 4f).

Visual comparison between the results of steerable filters (Fig. 4b and 4c) with the results of wavelet transform (Fig. 4d, 4e and 4f) reveals that the results obtained from steerable filters are more superior especially in term of curvilinear and circular features that were apparent on the steerable filters maps but missed to detect on the wavelet transform maps. We believe that most of the NW-SE lineation detected on the steerable filters and the wavelet transform maps (Fig. 4) are related to Laramide structures. The NE-SW trends are related to wrench faulting originating in the basement and reactivated periodically through the Phanerozoic. Although at this stage we were unable to relate the curvilinear and the circular features detected on the steerable filters (Figs. 4b and 4c) to the geology of the area we are trying to find their sources and their geological significance.

Conclusions

The results obtained in this test are very promising because we were able to map curvilinear and to some extent circular geological features that were difficult to map using other image enhancing techniques wavelet analysis. In addition to curvilinear and circular features, steerable filters are effective also in mapping lineaments. The lineaments detected by steerable filters appear to be very continuous and coherent in comparison to wavelet transform. Mapping geological features using steerable filters, if implemented, would be completely automated and therefore much faster and more cost-effective than manual techniques. The features mapped with steerable filters would provide interpreters with a comprehensive objective dataset of features to use in forming a robust structural interpretation of HRAM data.

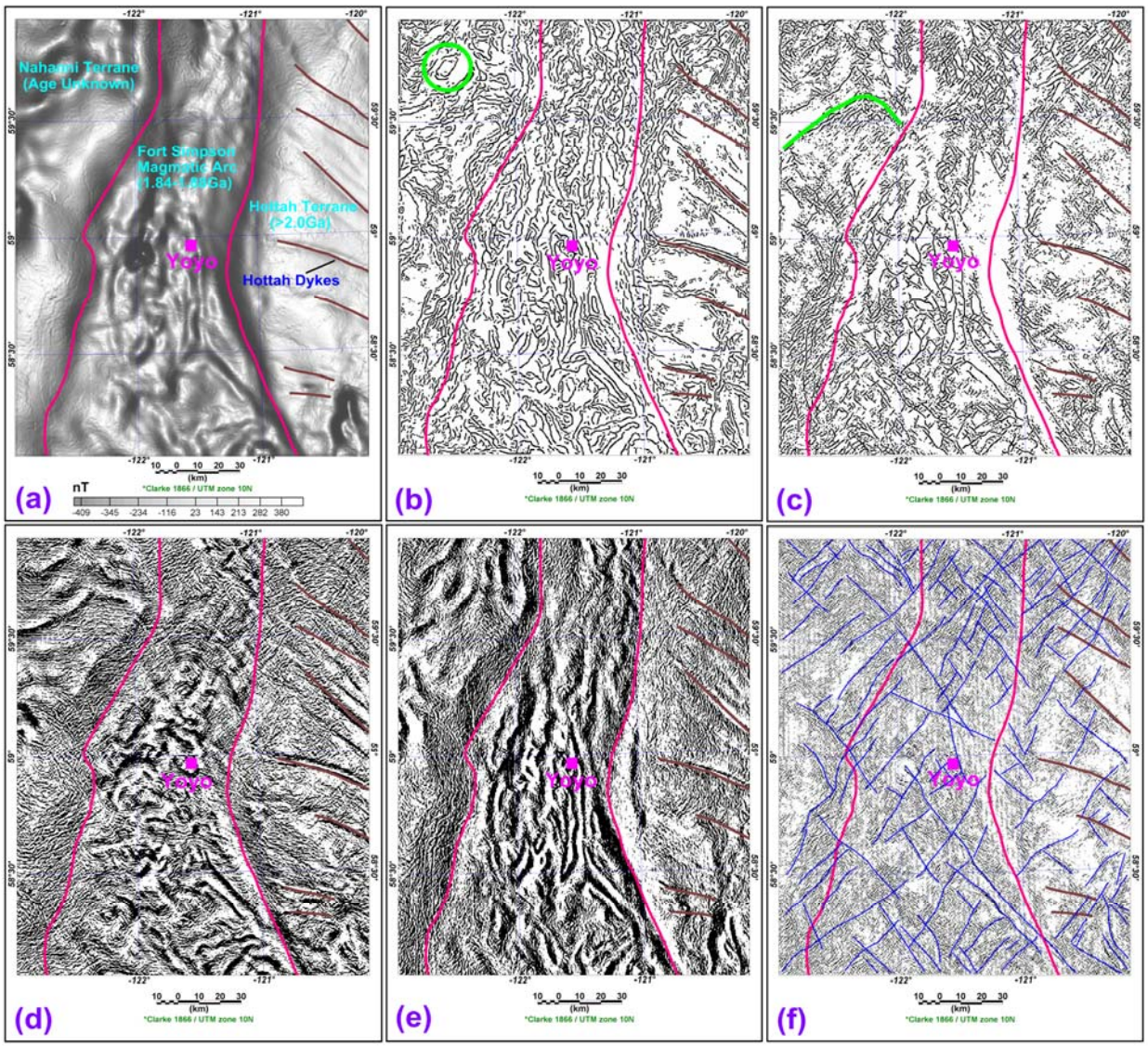

Figure 4. Results of steerable filters and 2-D wavelet transform; (a) reduced-to-pole total magnetic intensity grid; (b) results of steerable filters using the edge detector showing an example of a detected circular feature (green circle); (c) results of steerable filters using the ridge detector showing an example of a detected curvilinear feature (green polyline); (d) results of wavelet transform showing the horizontal information; (e) results of wavelet transform showing the vertical information; and (f) results of wavelet transform showing the diagonal information with interpreted lineaments plotted as blue lines.